Check for updates



www.chemcatchem.org

Better Together: Synergic Effect of Gallium-Based Catalyst and **Porous Support for Reduction Reactions**

Marco Aurelio Jiménez Sánchez, [a] Simon Carl, [b] Nicola Taccardi, [c] Marco Haumann, [d] Benjamin Apeleo Zubiri, [b] Peter Wasserscheid, [c, e] Erdmann Spiecker, [b] Nicolas Vogel, [f] Julien Bachmann, *[a] and Giulia Magnabosco*[f]

Liquid metal solutions are a new class of catalysts with outstanding properties in terms of catalytic conversion and resistance to coking. Finding the perfect combination of catalytic particles with homogeneous size distribution and support material able to stabilize them during catalysis is key for preparing model systems to gain understanding of these complex catalytic processes. In this work, we present a method for the preparation of small and narrowly distributed gallium-palladium particles supported on inverse opals, interconnected 3-D porous networks

with a very narrow pore size distribution. Our platform is a promising candidate as supported liquid metal catalytic system thanks to its permeability to fluids and its confined pore environment, which prevents the coalescence of the metal alloy, thus maximizing the surface area available for the catalytic reaction. We demonstrate their enhanced performance when compared to other state of the art systems giving a proof of concept of their application as catalysts for a simple model reaction, the reduction of methylene blue.

1. Introduction

Catalytically active liquid metal solutions, consisting of a metallic phase with low melting point containing a catalytic active

- [a] M. A. J. Sánchez, J. Bachmann Chair 'Chemistry of Thin Film Materials' (CTFM), Friedrich-Alexander University Erlangen-Nürnberg (FAU), IZNF, Cauerstraße 3, Erlangen 91058, Germany E-mail: julien.bachmann@fau.de
- [b] S. Carl, B. A. Zubiri, E. Spiecker Institute of Micro and Nanostructure Research (IMN) & Center for Nanoanalysis and Electron Microscopy (CENEM), Friedrich-Alexander University Erlangen-Nürnberg (FAU), IZNF, Cauerstraße 3, Erlangen 91058, Germany
- [c] N. Taccardi, P. Wasserscheid Lehrstuhl für Chemische Reaktionstechnik (CRT), Friedrich-Alexander University Erlangen-Nürnberg, (FAU), Egerlandstraße 3, Erlangen 91058, Germany
- [d] M. Haumann Research Centre for Synthesis and Catalysis, Department of Chemistry, University of Johannesburg, Auckland Park P.O. Box 524, South Africa
- [e] P. Wasserscheid Forschungszentrum Jülich GmbH, Helmholtz-Institute Erlangen-Nürnberg for Renewable Energy (IEK 11), Egerlandstraße 3, Erlangen 91058, Germany
- [f] N. Vogel, G. Magnabosco Institute of Particle Technology (LFG), Friedrich-Alexander-University Erlangen-Nürnberg (FAU), Cauerstraße 4, Erlangen 91058, Germany E-mail: giulia.magnabosco@fau.de
- Supporting information for this article is available on the WWW under https://doi.org/10.1002/cctc.202401429
- © 2024 The Author(s). ChemCatChem published by Wiley-VCH GmbH. This is an open access article under the terms of the Creative Commons Attribution-NonCommercial License, which permits use, distribution and reproduction in any medium, provided the original work is properly cited and is not used for commercial purposes.

metal, [1] have attracted growing interest in heterogeneous catalysis thanks to their uniform, single-atom catalytic centers that dynamically form by diffusion of the active species at the gas/liquid interface, and their efficiency in precious metal utilization.[2-4] In fact, the catalytically active liquid metal phase offers several attractive features: (i) a higher activity / selectivity because of the special nature of the atomically isolated active sites created in a liquid metal environment, [5] (ii) resistance to active metal agglomeration and thus constant catalyst performance, and (iii) self-healing properties and insensitivity to coking because of the high dynamics of the liquid interface. [6-9]

Supported catalytically active liquid metal solutions (SCALMS) consisting of palladium (Pd) as the catalytically active metal dispersed in gallium (Ga), the low melting point metallic phase, supported on porous glass, have been successfully prepared. [6,10] The metal alloy is stabilized on the surface of the porous structure and can be prepared either bottomup,^[6] obtaining the Ga phase by the thermal decomposition of molecular Ga precursors, or top down, using ultrasonication to obtain small Ga particles.[10-12] Furthermore, as the inclusion of the active metal is performed by galvanic displacement, a variety of active metals can be included in the system, opening the possibility to perform a great number of catalytically relevant reactions, such as the dehydrogenation of butane into butene. [6-8,13-15] The main drawback of both these systems consists of the low degree of control over the metal alloy size and distribution in within the support. In fact, producing the metal alloy using the top-down approach results in its agglomeration^[16] and localization on the support external surface, while using the bottom-up approach leads to coalescence and clogging of the internal pores. Furthermore, the limited interconnectivity of the pores in porous glass and aluminapreviously used as supports—reduces the reactants flow in the substrate and limits the exposure of the catalyst to them. In

Figure 1. Schematic representation of the proposed system. On the left, a representation of the previous generation of supports and metal alloys, where the difference in scale between the support pores and the metal alloy leads to an inefficient immobilization, and an SEM image of porous alumina previously used as support. On the right, a representation of the system suggested in this work and a representative SEM image of an inverse opal (IO). Here, the interconnected pores of the IOs structure are able to host isolated monodisperse metal alloy particles previously prepared using a novel hot-injection synthesis.

addition, the coalescence of Ga^[17] causes its escape from the substrate, thereby decreasing surface area and catalytic activity. All these features render the system more complicated to model and exploit efficiently, and thus less ideal for applications.

In this work, we aim at optimizing and gaining new understanding on the synergy between catalyst and support preparing a new generation of supported metal alloys by controlling their size and size distribution, and designing a support material that maximizes their exposure to reactants and minimizes coalescence (Figure 1).

The preparation of small and monodisperse Ga particles is a challenging task due to its high surface tension when in its pristine state, and its ease of oxidation.[17-19] The latter, despite threatening the life of the catalyst due to its solid nature and difficult reduction, can also be exploited to stop the growth of the metal alloy, prevent its coalescence and avoid further conversion into oxide.[20] Various methods for the preparation of Ga particles in the submicrometer range have been reported in the literature. [13,20-22] Here, we propose an adapted hot-injection synthesis method based on the degradation of GaH₃(quinuclidine). The hot injection method allows us to induce nucleation in a very short time span, favoring the formation of monodisperse particles, and to control their final size, e.g. by thermal quenching.^[23,24] By performing the synthesis in the presence of a catalytically active metal complex, it is possible to include the catalytically active element in the metal alloy. The one-step preparation of the Ga/Pd nanoparticles (hot-inj. Ga/Pd-NP) avoids the need for performing galvanic displacement to insert the catalysts in a second step. This facilitates the inclusion of the catalytically active metal specie in the alloy, as galvanic displacement poses several challenges and often gives rise to overgrowth of the second metal specie in a metal oxide shell around the actual Ga nanoparticle.[13,25] We selected Pd as the catalytically active metal for its relevance in industrial applications^[26,27] and for the ease of comparison to already reported Ga/Pd systems.[6]

Inverse opals (IOs), composed of a network of interconnected ordered pores in a continuous matrix prepared by using a template of sacrificial colloidal particles,^[28] are ideal as catalyst supports for their high surface area and allow for the flow of reactants and products. IOs containing catalytically active metal particles within the matrix or on its surface have been

successfully used for catalysis, proving the promising role of such a system in the field.^[29-32] In addition to the increase of active surface area, their application as supports for Ga/Pd also contributes to preventing coalescence of the metal alloy during the reaction. In atmospheric conditions, Ga possesses a layer of Ga oxide on its surface that prevents the metal alloy from merging. This layer needs to be reduced during catalysis, either by thermal treatment in vacuum or by acid or base treatment in solution, to expose the not oxidized Ga/Pd. IOs can prevent and/or limit coalescence as every pore acts as its own confined environment and the coalescence between particles in confining pores can be reduced due to the high surface tension of Ga. Silica was selected as the material for IOs as it has been shown to contribute to the selectivity of the catalyst in SCALMS systems and for its ability to withstand high temperature and harsh conditions.[8]

In this article, we present the use of IOs as supports for a Ga/Pd metal alloy synthesized using a newly established hot injection method, and demonstrate their synergy in the catalytic reduction of methylene blue (MB), used as a model catalytic reaction.

2. Results and Discussion

In a typical synthesis of hot-inj. GaPd-NP, a solution containing GaH_3 (quinuclidine) and $Pd(acac)_2$ is quickly injected in octadecene (ODE). Oleic acid (OA) is then added as a stabilizer and the reaction mixture is quickly cooled to room temperature and purified by a solvent-nonsolvent procedure.

The proposed method leads to the formation of GaPd nPs in the size range 12–32 nm, with an average size of 21 ± 4 nm (Figure 2a,b). The load of Pd can be controlled by changing the concentration of Pd(acac)₂ during the reaction. For this study, we selected a Pd loading of 5 wt.%.

The morphology and metal distribution in the particles were determined with TEM (Figure 2c-f). We observe that Pd is distributed in the particle, with a slight increase in its concentration on the particle surface. Furthermore, the distribution of Pd and Ga reported in Figure 2 and Table 1 is representative of the whole sample (Table SI1 and Figure SI1). The particles do not present any diffraction reflection in Powder X-Ray Diffraction (Figure



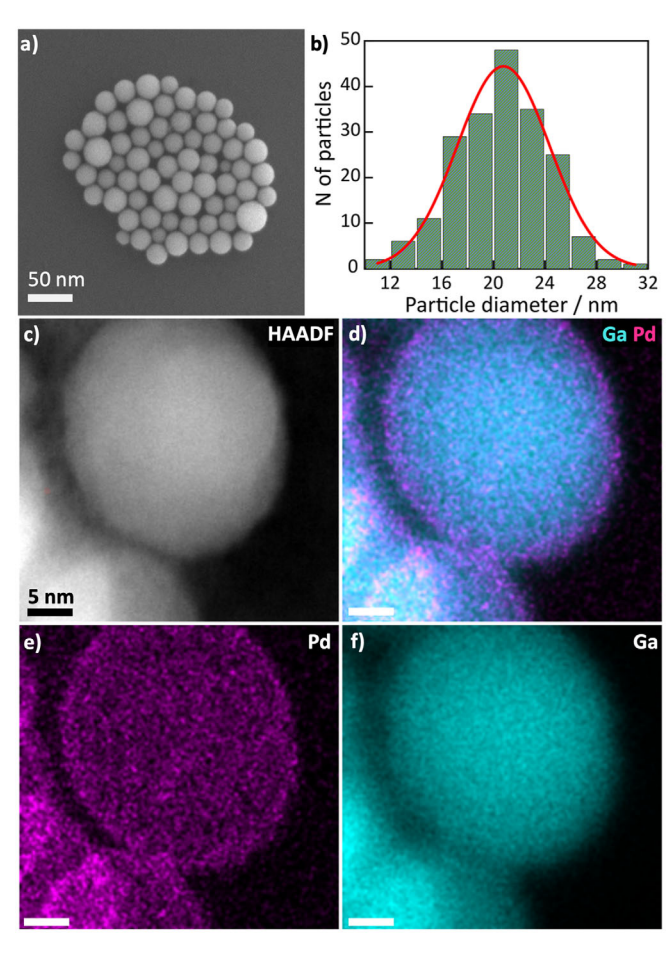


Figure 2. Characterization of the hot-inj. GaPd-NP. a) SEM micrograph and b) size distribution of the particles. c) TEM image and d-f) corresponding elemental distribution, visualized as net intensity.

Table 1. Pd and Ga content in hot-inj. GaPd-NP and Std. GaPd evaluated using EDS-SEM.			
	Ga (wt.%)	Pd (wt.%)	Particle Size (nm)
hot-inj. GaPd-NP	95.0 ± 1.0	5.0 ± 0.7	21 ± 4
Std. GaPd	97.8 ± 0.2	2.2 ± 0.1	\sim 500 \pm 200 ^[8]

SI2). Upon application of the catalyst in the envisioned dehydrogenation reactions carried out in the gas phase at elevated temperature, the phase diagram demonstrates that the particle will be homogeneously mixed and molten.^[6] Importantly, Pd is present inside the particle and not just segregated to a specific area.[25]

In the examples of IOs used as catalyst supports reported in the literature, IOs films prepared on a solid substrate with the colloidal coassembly method are used. [28-30,33] This method leads to highly ordered IOs with perfectly interconnected pores and few defects, but limits the amount of catalytic material to the layer deposited on the support. To increase the yield of the fabrication procedure and prepare a sufficient amount of material for catalytic tests (Figure SI3a), the preparation of free-standing IOs (FS-IOs) was optimized.[33] Here, IOs were prepared using the

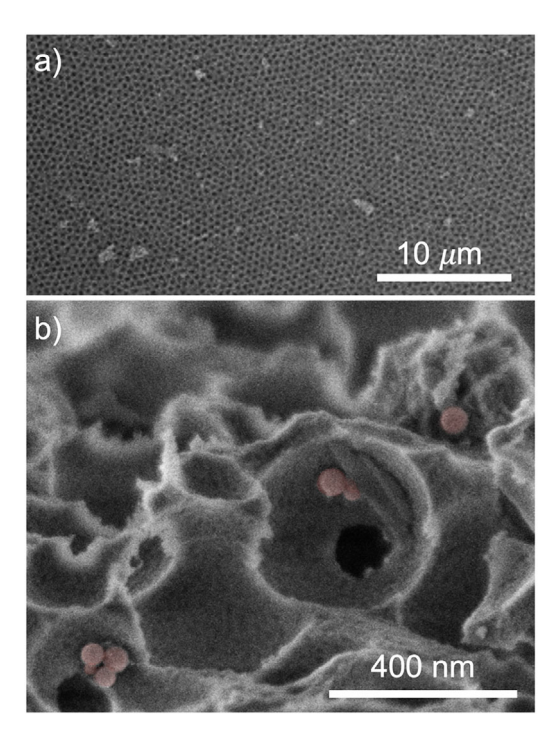


Figure 3. SEM images of free standing inverse opals loaded with hot-inj. GaPd-NP, a) Low magnification SEM image and b) high magnification side view SEM image of a FS IOs flake loaded with hot-inj. GaPd-NP, highlighted

vertical walls of the container as sacrificial supports. Despite the lower order of the pores of FS-IOs compared to IOs prepared on planar supports, the overall interconnectivity of the pores within the material is preserved (Figure 3a, Figure SI3b).

The lower degree of order is counteracted by the exposure of all the faces to the solution and does not affect the permeability of the IOs overall.

The hot-inj. GaPd-NP were loaded into the substrate by diffusion within the pores to reach a loading of 1 wt.% after careful washing with EtOH to remove the oleic acid shell.[20] While it would be possible to achieve higher loads, this would also favor coalescence and eventually decrease the catalytic efficiency. The loading process is performed at room temperature, thus not impacting the thickness of the oxide layer of GaPd-NPs. Here, the ability to control the cross-sections of the pores and necks connecting two adjacent pores is key to ensure an efficient exploitation of the entire surface area. We selected a pore size of \sim 550 nm, giving rise to a \sim 175 nm neck (Figure SI3c). This ensures the diffusion of the 20 nm particles through the whole support. The particles then settle on the inner surface of the IOs upon drying, as seen in Figure 3b. The oxide shell also prevents the coalescence of the hot-inj. GaPd-NP during this stage.

For the evaluation of the catalytic activity of hot-inj. GaPd-NP on inverse opals (hot-inj. GaPd-NP@IOs), we investigate the reduction of methylene blue to leuco-methylene blue (LMB), commonly used as a standard reaction to test reduction activity.[34] In this reaction, ascorbic acid acts as the reducing agent in the conversion of the colored MB to the colorless LMB. The reaction can be monitored by the decrease in absorbance at \sim 665 nm (Figure SI4 reports the decreased absorbance for all the

) on Wiley Online Library for rules of use; OA articles are governed by the applicable Creative Comn

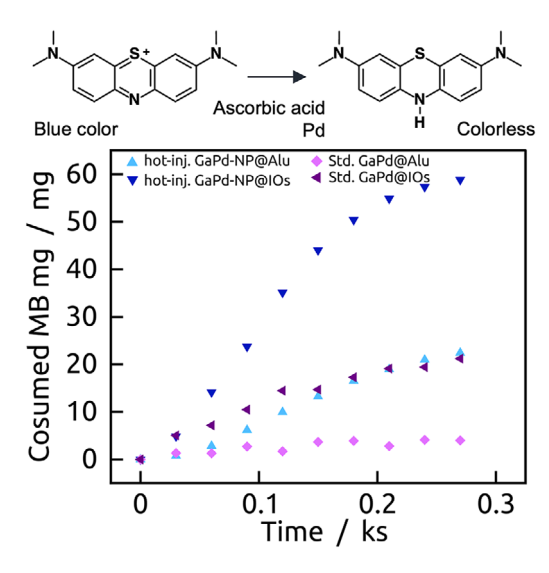


Figure 4. Evaluation of catalytic properties. Top: Reaction scheme of the reduction of methylene blue to leuco methylene blue, used as model reaction to evaluate the catalytic performances of the systems. Bottom: Catalytic performances in the reduction of methylene blue of hot-inj. GaPd-NP@IOs, Std. GaPd@IOs, hot-inj. GaPd-NP@Alu, and Std. GaPd@Alu.

investigated samples). As the reaction takes place in acidic environment (pH~2), the oxide layer is reduced while the reaction takes place.

We compared the catalytic activity of hot-inj. GaPd-NP and state-of-the-art GaPd particles synthesized by ultrasonication (Std. GaPd) as reported in the literature, [10,21] both on IOs (hot-inj. GaPd-NP@IOs and Std. GaPd@IOs) and on porous alumina (hotinj. GaPd-NP@Alu and Std. GaPd@Alu) (Figure 4, Figure SI7). Their composition and size are reported in Table 1.

In the absence of metal alloy, no MB conversion is observed (Figure SI5). Comparing Std. GaPd supported on porous alumina and on IO, we can see that the porous structure of the IO improves the catalytic performance of both systems. We ascribe this to the stabilization of the metal alloy by the surface porosity of the IO, which reduces coalescence.

When loaded on IOs, the conversion rate achieved with hotinj. GaPd-NP is significantly higher than that of Std. GaPd, the current state-of-the-art method for the preparation of this particular metal alloy. The higher surface area of the smaller particles provides higher activity than Std. GaPd. At the same time, as the metal alloy is confined in the pores of the IO, coalescence is reduced (Figure SI6). These observations confirm the advantage given by synergy between the hot-inj. GaPd-NP combined with a perfectly suited support when compared to Std. GaPd supported on a conventional, commercially available porous alumina support.

The confinement given by the IO structure prevents aggregation during the catalytic process, as observed in Figure 5.

3. Conclusions

In this article, we shed light on the combined effects of catalytic particle size and matching porous supports in supported

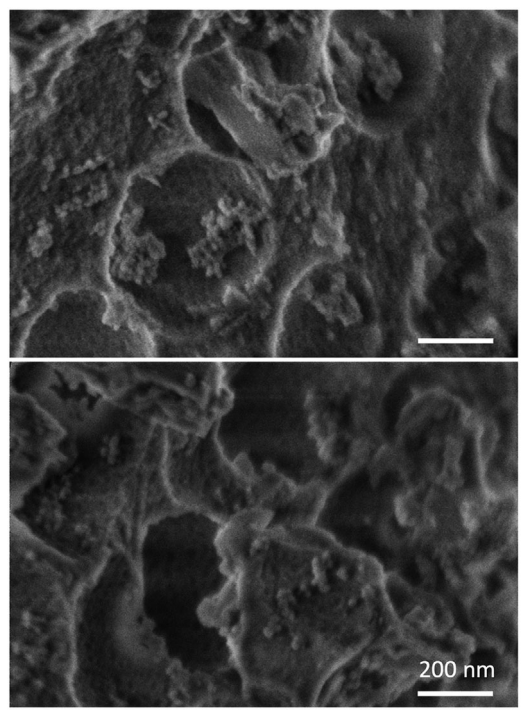


Figure 5. Morphology of hot-inj. GaPd-NP@IOs before and after catalytic tests, highlighting how the morphology is not impacted by the reaction. Top: SEM image of hot-inj. GaPd-NP@IOs before the catalytic test. Bottom: SEM image of hot-inj. GaPd-NP@IOs after the catalytic test.

catalytically active liquid metal systems. GaPd particles synthesized by a hot injection method with a narrow size distribution and supported on an inverse opal exhibit enhanced activity with respect to state-of-the-art systems. The highly porous supports with defined pore size and geometry give rise to an ideal synergy between the catalyst and the support, and thus provides a higher effective catalytic activity. Our findings highlight the contributions of the different components of such complex systems, and provides important fundamental understanding of the synergy between the components as a basis for their scale-up and application in industrially relevant reactions.

4. Experimental Section

4.1. Materials and Methods

Palladium (II) bis(acetylacetonate) [Pd(acac)₂], methylene blue (97%), 1-octadecene (ODE, 90%), oleic acid (OA, 90%), chloroform (CHCl₃, 99%) were purchased from Sigma-Aldrich; ethanol (>98%) was obtained from Carl Roth. All chemicals were used as received.

4.1.1. Synthesis of Hot-inj. GaPd-NP

 $H_3Ga(quinuclidine)$ was synthesized as described by Atwood et al and Greenwood et al.[35,36] In a glovebox, a precursor solution of Ga/Pd was prepared dissolving 25 mg of the GaH₃(quinuclidine) and 1.44 mg of Pd(acac)₂ in 6 mL of ODE, previously degassed and dried under vacuum at 110 °C for 4 h. To promote dissolution of precursors, the solution was ultrasonicated for 5 min, forming a pale-yellow

Europe

European Chemical Societies Publishing

Chemistry

solution, which indicated the complete dissolution of Ga and Pd

7 mL of ODE were loaded into a 50 mL three-neck roundbottom flask with a reflux condenser, a thermocouple attached to an adapter, a rubber septum, and a magnetic stir bar. The flask was degassed and dried under dynamic vacuum at a temperature of 110 °C for 1 h. The flask was cycled three times between vacuum and N₂ and heated to 280 °C under N₂-flow before injecting the Ga/Pd precursor described above. The temperature decreased to 225-230 °C. After 45 s at 240 °C, 1 mL of OA was added, quickly cooled down to room temperature by ice bath. To purify the products after the synthesis, hot-inj. GaPd-NP were precipitated by adding 10 mL of chloroform and 20 mL of ethanol, followed by centrifugation at 7500 RPM for 10 min. This process was repeated three more times. The hot-inj. Ga/Pd-NPs were redissolved in chloroform and stored under ambient conditions. Postsynthetic purification, handling, and storage of hot-inj. Ga/Pd-NPs were carried out under ambient conditions.

A JSM-F100 Field-Emission Scanning Electron Microscope manufactured by JEOL and equipped with an energy dispersive spectrometer (EDS-SEM) was used for the study of the morphology and composition of GaPd-NP with an acceleration voltage of 5–15 kV.

The diffractograms were obtained with a Bruker D8 ADVANCE instrument that incorporates a Cu K α source and a LYNXEYE XE-T

Scanning transmission electron microscopy (STEM) imaging with high-angle annular dark-field (HAADF) and STEM EDX analysis were performed in a double-aberration corrected FEI Titan Themis 300 transmission electron microscope with an accelerating voltage of 300 kV. STEM-EDXS measurements were acquired with 30 µs dwelltime and a probe current of 122-310 pA. The probe-forming semiangle was set to a value of 15.7 mrad. Spectrum image visualization and quantification was optimized with the help of Thermo Scientific Velox Software (3.8.1.14).

4.1.2. Inverse Opal Preparation

Inverse opals (IO) were synthesized using the colloidal coassembly method already reported in the literature. [28] First, polystyrene nanospheres were synthesized using the surfactant-free polymerization method using ammonium persulfate as initiation and acrylic acid as comonomer.[37] 1 mL of tetraethyl orthosilicate (TEOS) was hydrolyzed by using 1 mL of 0.1 N HCl in the present of 1.5 mL of EtOH under stirring for 1 h. After hydrolysis, 75 μL of the TEOS solution was added to 12 mL of 0.1 wt.% dispersion of polystyrene nanoparticles in a glass container. The solution was evaporated at 65 °C over 5 days. The residual material was then calcined under air atmosphere to remove the organic template using the following ramp: room temperature (RT) to 500 °C in 5 h, 2 h at 500 °C followed by natural cooling. The free-standing inverse opal was then collected from the vial and used as is without further processing (e.g. crushing). The loading was performed right after the collection of the samples, and the samples were kept under air in the dark until then.

The IOs were characterized using a Zeiss Gemini 500 working at 1 kV, equipped with an Inlens detector.

4.1.3. Catalyst Loading Onto Support

In a typical loading experiment, 0.3 mg of metal alloy dispersed in CH₃Cl was added to 10 mg of support in air atmosphere at room temperature. The reaction was sonicated for 5 min while manually shaken to prevent sedimentation and the solvent was removed by sparging N₂ to the flask. The samples were then directly used for the catalytic tests. The metal alloys loaded onto the supports were characterized using a Zeiss Gemini 500 working at 1 kV, equipped with an Inlens detector.

Samples were prepared using hot-inj. GaPd-NP and freestanding IOs were synthesized as described above, Std. Ga/Pd was prepared using ultrasonication, as reported in the literature, [10] and commercially available alumina support, using the just mentioned protocol.

4.1.4. Catalytic Activity Measurements

Methylene blue (97%), ascorbic acid (99%), and HCl (1 M) were purchased from Sigma-Aldrich and used as received.

In a typical measure, the sample was first added to a quartz microcuvette. 635 µL of water, 2.5 µL of 1 mg/mL ascorbic acid solution, and 25 µL of 0.1 mg/mL of methylene blue solution were added to the cuvette. The solution was quickly stirred and the UV-vis spectra was recorded every minute using a OceanOptics DH-2000-BAL deuterium/alogen source and a OceanOptics HR4000 Spectrometer.

Supporting Information

Details on the synthesis of Ga/Pd particles and their characterization, the fabrication of IOs and their characterization, and additional details on the catalytic tests are reported in the Supporting Information. The raw data can be found at https://doi. org/10.5281/zenodo.13268474.

Author Contributions

Marco Aurelio Jiménez Sánchez developed the synthesis of hotinj. GaPd-NP and performed SEM characterization, loaded the catalysts on the supports and conducted the catalytic tests, supervised by Julien Bachmann. Simon Carl performed TEM characterization, supervised by Benjamin Apeleo Zubiri and Erdmann Spiecker. Nicola Taccardi synthesized GaH₃(quinuclidine), supervised by Marco Haumann and Peter Wasserscheid. Giulia Magnabosco prepared and characterized the IOs with the supervision of Nicolas Vogel. Giulia Magnabosco wrote the manuscript. Marco Aurelio Jiménez Sánchez, Nicolas Vogel, Julien Bachmann and Giulia Magnabosco conceptualized the research. Giulia Magnabosco, Julien Bachmann, Nicolas Vogel, Marco Haumann, Peter Wasserscheid and Erdmann Spiecker provided the funding for carrying out the project. All the authors approved the final version of the manuscript.

Acknowledgements

Giulia Magnabosco acknowledges funding from "Bavarian Equal Opportunities Sponsorship - Realisierung von Frauen in Forschung und Lehre (FFL) - Promotion Equal Opportunities for Women in Research and Teaching.". All the authors acknowledge the Deutsche Forschungs gemeinschaft (DFG, German Research Foundation) - Project-ID 431791331-SFB 1452. Giulia Magnabosco and Nicolas Vogel acknowledge the DFG project BA4277-16/1

Chemistry Europe

European Chemical Societies Publishing

and project VO 1824/9–1. Marco Aurelio Jiménez Sánchez and Julien Bachmann acknowledge the German Ministry of Education and Research (BMBF)-project "Tubulyze" (project number 03SF0564A).

Open access funding enabled and organized by Projekt DEAL.

Conflict of Interests

The authors declare no conflict of interest.

Data Availability Statement

The data that support the findings of this study are openly available in Zenodo at https://doi.org/10.5281/zenodo.13268473, reference number 13268473.

Keywords: Catalysis · Gallium · Inverse opal · Liquid metal · Palladium

- M. Ameen, F. Jabbar, D. Yang, M. Irfan, V. Krishnamurthi, C. J. Parker, K. Zuraiqi, T. C. Le, M. J. S. Spencer, T. Daeneke, K. Chiang, *ChemCatChem* 2023, 15, e202300814.
- [2] F.-M. Allioux, M. B. Ghasemian, W. Xie, A. P. O'Mullane, T. Daeneke, M. D. Dickey, K. Kalantar-Zadeh, *Nanoscale Horiz.* 2022, 7, 141–167.
- [3] S. S. Fatima, K. Zuraiqi, A. Zavabeti, V. Krishnamurthi, K. Kalantar-Zadeh, K. Chiang, T. Daeneke, Nat. Catal. 2023, 6, 1131–1139.
- [4] T. Daeneke, K. Khoshmanesh, N. Mahmood, I. A. de Castro, D. Esrafilzadeh, S. J. Barrow, M. D. Dickey, K. Kalantar-zadeh, Chem. Soc. Rev. 2018, 47, 4073–4111.
- [5] F. Zhang, Y. Zhu, Q. Lin, L. Zhang, X. Zhang, H. Wang, Energy Environ. Sci. 2021, 14, 2954–3009.
- [6] N. Taccardi, M. Grabau, J. Debuschewitz, M. Distaso, M. Brandl, R. Hock, F. Maier, C. Papp, J. Erhard, C. Neiss, W. Peukert, A. Görling, H.-P. Steinrück, P. Wasserscheid, *Nature Chem* 2017, 9, 862–867.
- [7] H. Wittkämper, R. Hock, M. Weißer, J. Dallmann, C. Vogel, N. Raman, N. Taccardi, M. Haumann, P. Wasserscheid, T.-E. Hsieh, S. Maisel, M. Moritz, C. Wichmann, J. Frisch, M. Gorgoi, R. G. Wilks, M. Bär, M. Wu, E. Spiecker, A. Görling, T. Unruh, H.-P. Steinrück, C. Papp, Sci. Rep. 2023, 13, 4458.
- [8] N. Raman, M. Wolf, M. Heller, N. Heene-Würl, N. Taccardi, M. Haumann, P. Felfer, P. Wasserscheid, ACS Catal. 2021, 11, 13423–13433.
- [9] M. Wolf, N. Raman, N. Taccardi, M. Haumann, P. Wasserscheid, *Chem-CatChem* 2020, *12*, 1085–1094.
- [10] N. Raman, J. Söllner, N. Madubuko, S. Nair, N. Taccardi, M. Thommes, M. Haumann, P. Wasserscheid, Chem. Eng. J. 2023, 475, 146081.
- [11] Y. Lin, J. Genzer, W. Li, R. Qiao, M. D. Dickey, S.-Y. Tang, *Nanoscale* 2018, 10, 19871–19878.
- [12] V. B. Kumar, A. Gedanken, Z. Porat, *Ultrason. Sonochem.* 2023, 95, 106364.

- [13] L. Castilla-Amorós, D. Stoian, J. R. Pankhurst, S. B. Varandili, R. Buonsanti, J. Am. Chem. Soc. 2020, 142, 19283–19290.
- [14] D. Esrafilzadeh, A. Zavabeti, R. Jalili, P. Atkin, J. Choi, B. J. Carey, R. Brkljača, A. P. O'Mullane, M. D. Dickey, D. L. Officer, D. R. MacFarlane, T. Daeneke, K. Kalantar-Zadeh, *Nat. Commun.* 2019, *10*, 865.
- [15] M. Armbrüster, G. Wowsnick, M. Friedrich, M. Heggen, R. Cardoso-Gil, J. Am. Chem. Soc. 2011, 133, 9112–9118.
- [16] S. Ki, J. Shim, S. Oh, E. Koh, D. Seo, S. Ryu, J. Kim, Y. Nam, Int. J. Heat Mass Transfer 2021, 170, 121012.
- [17] Y. Ding, M. Zeng, L. Fu, Matter 2020, 3, 1477–1506.
- [18] S.-Y. Tang, C. Tabor, K. Kalantar-Zadeh, M. D. Dickey, Annu. Rev. Mater. Res. 2021, 51, 381–408.
- [19] K. Kalantar-Zadeh, J. Tang, T. Daeneke, A. P. O'Mullane, L. A. Stewart, J. Liu, C. Majidi, R. S. Ruoff, P. S. Weiss, M. D. Dickey, ACS Nano 2019, 13, 7388–7395.
- [20] V. Okatenko, L. Castilla-Amorós, D. C. Stoian, J. Vávra, A. Loiudice, R. Buonsanti, J. Am. Chem. Soc. 2022, 144, 10053–10063.
- [21] O. Sebastian, A. Al-Shaibani, N. Taccardi, U. Sultan, A. Inayat, N. Vogel, M. Haumann, P. Wasserscheid, Catal. Sci. Technol. 2023, 13, 4435–4450.
- [22] Y. Lin, J. Genzer, M. D. Dickey, Adv. Sci. 2020, 7, 2000192.
- [23] C. B. Murray, C. R. Kagan, M. G. Bawendi, Annu. Rev. Mater. Sci. 2000, 30, 545–610.
- [24] V. K. Lamer, R. H. Dinegar, J. Am. Chem. Soc. 1950, 72, 4847–4854.
- [25] S. Carl, J. Will, N. Madubuko, A. Götz, T. Przybilla, M. Wu, N. Raman, J. Wirth, N. Taccardi, B. A. Zubiri, M. Haumann, P. Wasserscheid, E. Spiecker, J. Phys. Chem. Lett. 2024, 15, 4711–4720.
- [26] X. Wu, H. Neumann, M. Beller, ChemSusChem 2013, 6, 229-241.
- [27] C. Torborg, M. Beller, Adv. Synth. Catal. 2009, 351, 3027–3043.
- [28] B. Hatton, L. Mishchenko, S. Davis, K. H. Sandhage, J. Aizenberg, Proc. Natl. Acad. Sci. U.S.A. 2010, 107, 10354–10359.
- [29] A. Filie, T. Shirman, M. Aizenberg, J. Aizenberg, C. M. Friend, R. J. Madix, Catal. Sci. Technol. 2021, 11, 4072–4082.
- [30] A. Filie, T. Shirman, A. C. Foucher, E. A. Stach, M. Aizenberg, J. Aizenberg, C. M. Friend, R. J. Madix, J. Catal. 2021, 404, 943–953.
- [31] J. E. S. van der Hoeven, A. V. Shneidman, N. J. Nicolas, J. Aizenberg, Acc. Chem. Res. 2022, 55, 1809–1820.
- [32] J. H. Han, A. V. Shneidman, D. Y. Kim, N. J. Nicolas, J. E. S. Van Der Hoeven, M. Aizenberg, J. Aizenberg, Angew Chem Int Ed 2022, 61, e202111048.
- [33] K. R. Phillips, G. T. England, S. Sunny, E. Shirman, T. Shirman, N. Vogel, J. Aizenberg, Chem. Soc. Rev. 2016, 45, 281–322.
- [34] M.d. A. Rahim, J. Tang, A. J. Christofferson, P. V. Kumar, N. Meftahi, F. Centurion, Z. Cao, J. Tang, M. Baharfar, M. Mayyas, F.-M. Allioux, P. Koshy, T. Daeneke, C. F. McConville, R. B. Kaner, S. P. Russo, K. Kalantar-Zadeh, *Nat. Chem.* 2022, *14*, 935–941.
- [35] J. L. Atwood, S. G. Bott, F. M. Elms, C. Jones, C. L. Raston, *Inorg. Chem.* 1991, 30, 3792–3793.
- [36] N. N. Greenwood, A. Storr, J. Chem. Soc. 1965, 3426.
- [37] N. Vogel, L. de Viguerie, U. Jonas, C. K. Weiss, K. Landfester, Adv. Funct. Mater. 2011, 21, 3064–3073.

Manuscript received: August 16, 2024 Revised manuscript received: November 14, 2024 Accepted manuscript online: November 14, 2024 Version of record online: December 07, 2024